

Unbalanced wind buffeting effects on bridges during double cantilever erection stages

Pedro A. Mendes[†] and Fernando A. Branco[‡]

ICIST, Department of Civil Engineering, IST, Av. Rovisco Pais, 1096 Lisbon, Portugal

Abstract. This paper is focused on the torsional effects that are induced on bridge piers by unbalanced wind buffeting on the deck during double cantilever erection stages. The case of decks with variable cross section is considered in particular as this characteristic is typical of most frame bridges that are built by the cantilever method. The procedure outlined in the paper is basically an application of the method that Dyrbye and Hansen (1996) have illustrated for decks with constant cross section. This format was chosen because it is suitable for design purposes and may easily be implemented in structural codes. As a complement, the correspondence with the format that is adopted in the Canadian code (NBCC 1990) for the gust factor is established, which might be useful to bridge designers used to the North-American approach to the gust effects on structures. Only alongwind turbulence and horizontal movements of the deck are considered. The combination of torsional and bending effects is also discussed and it is illustrated with an example of application.

Key words: bridges; alongwind effects; torsion of piers; combined bending and torsion; cantilever erection stages.

1. Introduction

The effects of wind buffeting on bridges during the erection of the deck by the double cantilever method should be assessed by designers. In fact, the flexibility that bridge structures usually present at these erection stages may lead to undesirable stresses and displacements under the random excitation due to wind gusts. The use of temporary cables is often adopted as a remedy for such effects. Some examples of application of this solution are the Mezcala Bridge (Revelo *et al.* 1994), the Glebe Island Bridge (Wheeler *et al.* 1994), the Pasco-Kennewick Bridge and the Talmadge Memorial Bridge (Tang 1994).

As mentioned by Davenport (1994), the torsional effects due to unbalanced wind buffeting were first considered by Sir Benjamin Baker in the design of the Firth of Forth Bridge. He then assumed a rule-of-thumb in the design of the piers—simply “full mean wind” on one overhang and “no wind” on the other. A pioneering procedure to evaluate the torsional effects induced by wind gusts on a cantilever bridge was given by Davenport (1967), but only the resonant component of the torque was then considered and the influence of the cross section being variable was not investigated. The torsional effects of wind gusts were also studied by Foutch and Safak (1981), but only building-type structures (i.e., not bridges) were considered.

The unbalanced wind loading on double cantilever bridges was recognised by the ASCE Committee on Loads and Forces on Bridges as a subject for which additional investigation and

[†] Associate Professor

[‡] Professor

development of guidelines would be useful (“Bridge loading: research needed” 1982). This particular wind loading has been considered in the ECCS Recommendations 1989, but the application of the method given there is somewhat intricate and hardly compatible with the design practice. The latest version of Eurocode 1 (EC1 1995) does not supply any information about this phenomenon. Recently, Dyrbye and Hansen (1996) presented the torsional effects on cantilever bridges in a format suitable for design purposes and illustrated it to the case of a deck with constant cross-section.

This paper is focused on the torsional effects induced on cantilever bridges that present a deck with variable depth and on the joint analysis of bending and torsional effects. The importance of torsion is illustrated and it is shown that the gust factor on these bridges (regarding the bending and torsional effects) may be evaluated as if the depth of the deck were constant, since the error involved in this approximation has little significance.

The method illustrated in this paper is suitable for design practice and for implementation in codes. The method is first given in the Dyrbye and Hansen's format and the correspondence with the format that is adopted in the Canadian code (NBCC 1990) for the evaluation of the structural effects of wind gusts is then established. Only alongwind turbulence and horizontal movements of the deck are considered. The unbalanced wind loads that may arise from vertical turbulence, vortex shedding phenomena, special local topographic conditions or from structural asymmetry are not taken into account.

The paper consists of six main parts:

- (1) a brief review of the standard gust factor method, presented for the sake of clarity and illustrated with alongwind bending effects,
- (2) the modifications needed to apply this method for the torsional effects on cantilever bridges,
- (3) analysis of decks with variable cross section,
- (4) correspondence with the NBCC format,
- (5) joint analysis of bending and torsional effects and
- (6) an example of application.

2. Alongwind response of line-like structures

On a line-like structure with total length L and with linear-elastic behavior, any structural response (R) due to the drag force that is induced by the mean wind speed is given by :

$$\mu_R = \int_0^L \frac{1}{2} \rho U^2(s) D(s) C_D(s) I_R(s) ds = \left(\frac{1}{2} \rho U_{ref}^2 D_{ref} C_{D.ref} \right) I_{R.ref} \gamma_m L \quad (1)$$

where ρ is the specific mass of the air, U is the mean wind speed, D and C_D denote a reference dimension and the drag coefficient of the cross section of the structure, s corresponds to the coordinate along the length of the structure and $I_R(s)$ is the structural response due to a static unit load applied at section with coordinate s . The subscript “*ref*” denotes a reference value (such as the value at a reference section of the structure, located at height z_{ref} above the ground) and the γ_m -function is defined by:

$$\gamma_m = \frac{1}{L} \int_0^L g_m(s) ds \quad (2)$$

$$g_m(s) = \left(\frac{U(s)}{U_{ref}} \right)^2 \frac{D(s) C_D(s) I_R(s)}{D_{ref} C_{D.ref} I_{R.ref}} \quad (3)$$

This paper is devoted to buffeting effects on bridges, so that only horizontal structures are addressed for. Thus, z_{ref} corresponds to the height of the bridge deck above ground and terms like $U(s)/U_{ref}$ are unitary. Nevertheless, the general format of the equations will be retained, for the sake of completeness.

Assuming that U is much larger than the longitudinal fluctuations of wind speed and than the velocity of structural oscillation, the response μ_R may be taken as the mean response due to the wind action. On the other hand, the mean of the largest values of the response that occur during time intervals with a pre-defined duration T (usually 10 minutes) is called the characteristic response, R_k , and may be expressed in the form :

$$R_k = \mu_R + \kappa \sigma_R \quad (4)$$

where σ_R is the standard deviation of the response fluctuations and κ is the so-called peak factor. The variance of the response is usually split in two terms, namely the background and the resonant components (denoted by σ_b^2 and σ_r^2 , respectively). These two separate contributions may be presented in the form (Dyrbye and Hansen 1996) :

$$\sigma_b = \mu_R (2I_{u.ref}) \frac{1}{\gamma_m} \sqrt{v_b} \quad (5a)$$

$$\sigma_r = \mu_R (2I_{u.ref}) \frac{1}{\gamma_m} \sqrt{v_r} \quad (5b)$$

where $I_{u.ref} (= \sigma_{u.ref}/U_{ref})$ is the intensity of longitudinal turbulence at height z_{ref} and the non-dimensional variances v_b , v_r are defined in the following. If the mean response is not zero, the so-called gust factor (φ) is defined such that $R_k = \varphi \mu_R$. From the previous equations, it follows that :

$$\varphi = 1 + \kappa \sigma_R / \mu_R = 1 + \kappa (2I_{u.ref}) \frac{1}{\gamma_m} \sqrt{v_b + v_r} \quad (6)$$

If the quasi-static model is assumed for the background turbulence effects, the non-dimensional variance v_b (also indicated by J_b^2) is given by :

$$v_b = J_b^2 = \frac{1}{L} \int_0^L \int_0^L g_b(s_1) g_b(s_2) \rho_u(|s_1 - s_2|) ds_1 ds_2 \quad (7)$$

$$g_b(s) = \frac{U(s) D(s) C_D(s) I_R(s) \sigma_u(s)}{U_{ref} D_{ref} C_{D.ref} I_{R.ref} \sigma_{u.ref}} \quad (8)$$

The function ρ_u is the correlation coefficient of the longitudinal fluctuations of wind speed and it is related with the lateral length scale of longitudinal turbulence (L_u^y). Assuming that :

$$\rho_u(r) = \exp\left(-\phi_b \frac{r}{L}\right) \quad (9)$$

where $r = |s_1 - s_2|$ and ϕ_b is defined through :

$$\phi_b = \frac{L}{L_u^y(z_{ref})} \quad (10)$$

the double integral in Eq. (7) can be solved by (Dyrbye and Hansen 1996) :

$$J_b^2 = \frac{1}{L} \int_0^L G_b(r) \rho_u(r) dr \quad (11)$$

$$G_b(r) = \frac{2}{L} \int_0^{L-r} g_b(s) g_b(s+r) ds \quad (12)$$

Regarding the resonant turbulence effects for a particular structural mode of vibration, with natural frequency f_e (expressed in Hz), modal shape $\Phi(s)$ and total viscous damping δ (logarithmic decrement), the variance v_r is given by :

$$v_r = \left(\frac{M_1}{M_2} \right)^2 \frac{\pi^2}{2\delta} E(z_{ref}, f_e) J_r^2(f_e) \quad (13)$$

where M_1 and M_2 depend on the mass of the structure per unit span (denoted by m), $E(z, f_e) = f_e S_u(z, f_e) / \sigma_u^2(z)$ is the non-dimensional power spectrum of the along-wind turbulence and $J_r^2(f_e)$ is the joint-acceptance function. The following definitions apply :

$$M_1 = \int_0^L m(s) \frac{\Phi(s) I_R(s)}{\Phi_{ref} I_{R.ref}} ds \quad (14)$$

$$M_2 = \int_0^L m(s) \frac{\Phi^2(s)}{\Phi_{ref}^2} ds \quad (15)$$

$$J_r^2(f_e) = \frac{1}{L^2} \int_0^L \int_0^L g_r(s_1, f_e) g_r(s_2, f_e) \psi_F(|s_1 - s_2|, f_e) ds_1 ds_2 \quad (16)$$

$$g_r(s, f_e) = \frac{U(s) D(s) C_D(s) \Phi(s)}{U_{ref} D_{ref} C_{D.ref} \Phi_{ref}} \sqrt{\frac{S_u(s, f_e)}{S_{u.ref}(f_e)}} \quad (17)$$

where the function $\psi_F(r, f_e)$ is the normalized cross-spectrum of the fluctuations of the wind force. For horizontal structures, irrespective of the response being considered, $g_m(s) = g_b(s)$; besides, if $I_R(s) = \Phi(s)$ then $g_b(s) = g_r(s)$. Assuming that :

$$\psi_F(r, f_e) = \exp\left(-\phi_r \frac{r}{L}\right) \quad (18)$$

the double integral in Eq. (16) can be solved as for J_b^2 , i.e., through Eq. (11) with ρ_u replaced by ψ_F and with G_b replaced by a function (denoted by G_r) that is defined by Eq. (12) with g_r instead of g_b . The coefficient ϕ_r is usually expressed in the form :

$$\phi_r = \frac{C_r f_e L}{U_{ref}} \quad (19)$$

where C_r is a non-dimensional decay coefficient for which a wide variety of values may be found in the literature. For horizontal slender structures, located at a height H above ground, Solari (1987) indicates a mean value $C_r = 8.5 (L/H)^{0.25}$ and a range of variation given by :

$$5.0 \left(\frac{L}{H} \right)^{0.25} \leq C_r \leq 12.1 \left(\frac{L}{H} \right)^{0.25} \quad (20)$$

In Eurocode 1 it is implicit that C_r may be taken as 11.5 (following Solari 1987, 1993). However, it should be noted that this assumption is more appropriate for upright structures than for horizontal slender ones, such as bridge decks.

Regarding the peak factor, if the wind load is assumed to be a Gaussian stationary stochastic process and if the structural behavior is linear-elastic with viscous damping, κ may be evaluated by :

$$\kappa = \sqrt{2 \ln(vT)} + \frac{0.5772}{\sqrt{2 \ln(vT)}} \quad (21)$$

where ν is the zero-upcrossing frequency. Several approximate expressions for ν may be found in the literature. As the representative frequency of the background component is typically much lower than the structural one, it is common to consider the following expression (NBCC 1990) :

$$\nu = f_e \sqrt{\frac{\nu_r}{\nu_b + \nu_r}} \quad (22)$$

The present paper is focused on double cantilever bridges. The effects of wind gusts are evaluated according to the model shown in Fig. 1, that consists of two symmetric overhangs, each one with length $L/2$, supported on a vertical pier. The height of the deck above ground (H) is taken as constant and is defined at the centre point of the deck at the tip of each overhang. The reference cross section of the structure is chosen as one of the tips of the overhangs.

The structural behavior is assumed to be linear-elastic with viscous damping and no modal coupling is considered. The frequencies of the first modes of vibration that involve either alongwind bending or torsion of the pier are denoted by f_b and f_t , respectively; in both these modes of vibration, the deck is assumed to behave like a rigid body.

The net drag force on the whole deck (denoted by F) plays a crucial role among the alongwind effects in cantilever bridges. In practical cases, regarding the bending moment at the base or the

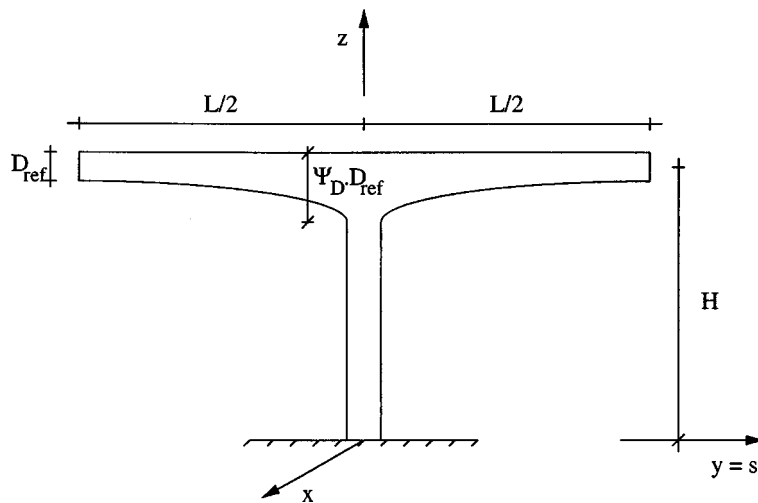


Fig. 1 Double cantilever bridge

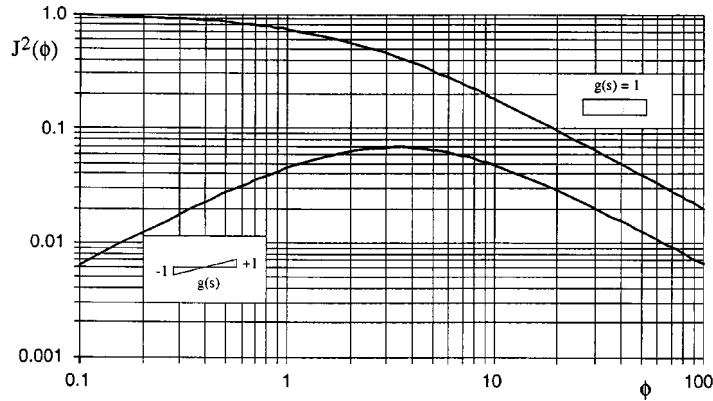


Fig. 2 Non-dimensional variance for a deck with constant cross section

alongwind displacement at the top of the pier, for instance, the contribution from drag induced by the pier is much less than the contribution from drag acting on the deck. Thus, if the effects of the “pier-drag” are neglected, the characteristic bending moments or alongwind displacements on the pier may be estimated by a static analysis of the structure, subjected to the characteristic force F_k at the top of the pier.

To evaluate F_k the corresponding unit load-response function (I_R) is unitary. The shape of the bending mode of vibration along the deck, $\Phi(s)$, is also unitary, as a result of the rigid behavior of the deck. Thus, it follows that $M_1 = M_2$. Furthermore, in the case of a deck with constant cross section, $g_m(s) = g_b(s) = g_r(s) = \gamma_{mF} = 1$. For an unitary g -function (either g_b or g_r), the Eqs. (11)-(12) lead to the following expression for the J^2 -function :

$$J^2(\phi) = \frac{2}{\phi^2}[\phi + \exp(-\phi) - 1] \quad (23)$$

This function is illustrated in Fig. 2. The monotonical decrease of the J^2 -function with ϕ reflects the loss of correlation on the wind force fluctuations with increasing span.

3. Torsional response of a double cantilever bridge

The standard ϕ method cannot be used directly to evaluate the torsional effects in the case of a cantilever bridge with symmetric overhangs, since the mean torsional moment (μ_T) is zero. However, to circumvent this difficulty, the torsional moment that is induced by mean wind load acting on only one of the overhangs may be considered instead of μ_T , i.e. :

$$\mu_{Th} = \int_0^{L/2} \frac{1}{2} \rho U^2(H) D(s) C_D(s) I_R(s) ds \quad (24)$$

where the subscript “ h ” stands for “half-deck”. Then, it is simple to verify that the characteristic torsional moment may be obtained through (Dyrbye and Hansen 1996) :

$$T_k = k \sigma_T = \phi \mu_{Th} \quad (25)$$

where :

$$\phi = \kappa(2I_{u.ref}) \frac{1}{\gamma_{mh}} \sqrt{v_b + v_r} \quad (26)$$

$$\gamma_{mh} = \frac{1}{L} \int_0^{L/2} g_m(s) ds \quad (27)$$

The variances v_b and v_r are still evaluated by Eq. (11) (either with G_b or G_r). However, as the origin of the s -axis is not located at one tip of the structure but rather at the middle (Fig. 1), a proper redefinition of the G -functions (instead of Eq. 12) is needed, namely :

$$G(r) = \frac{2}{L} \int_{-L/2}^{L/2-r} g(s)g(s+r)ds \quad (28)$$

To evaluate the torsional moment, the unit load-response function is $I_R(s) = s$; moreover, the torsional mode is assumed to be linear and anti-symmetrical about the pier, i.e., $\Phi(s) = s = I_R(s)$. Thus, it follows that $g_b(s) = g_r(s)$ and $M_1 = M_2$.

In the case of a deck with constant cross section, all the g -functions are given by $g(s) = 2s/L$ and the corresponding result $\gamma_{mh} = 1/4$ is obtained. Regarding the non-dimensional response variances, the Eqs. (11) and (28) lead to the following expression :

$$J^2(\phi) = \frac{8}{\phi^4} \left[\frac{\phi^3}{12} - \frac{\phi^2}{4} + 1 - \left(1 + \frac{\phi}{2} \right)^2 \exp(-\phi) \right] \quad (29)$$

Fig. 2 also illustrates this J^2 -function and shows that the largest variances for torsion correspond to the range $3 < \phi < 4$ (the maximum value is attained at $\phi \approx 3.4$). Thus, regarding the gust factor for the torsional effects, the critical span range is $L = [3 \text{ to } 4]$. $L_u^y(H)$ for the background turbulence effects and $L = [3 \text{ to } 4]$. $U(H)/(f_t, C_r)$ for the resonant component. Spans outside these ranges present less torsional effects: in longer spans due to the loss of correlation between the wind force fluctuations, and in shorter spans because both overhangs become fully enveloped by the relevant wind gusts.

Other torsional effects may be evaluated besides the moment that is induced on the pier. The alongwind displacement of the deck at the end of each overhang due to the torsion of the pier (Δ), for instance, is equal to $L/2$ times the pier rotation at the top. As the modal shape is defined through $\Phi(s) = s$ (i.e., it is normalized by the condition of unit rotation at the top of the pier), the rotation at the top corresponds directly to the ratio between the torsional moment and the modal stiffness. From these considerations, the characteristic value of Δ is given by :

$$\Delta_k = L/2 \frac{T_k}{(2\pi f_t)^2 \int_{-L/2}^{L/2} m(s)s^2 ds} \quad (30)$$

4. Deck with variable cross section

The decks of frame bridges built by the cantilever method often present a variable depth. This variation is usually parabolic with zero slope at mid-span. If the most unfavourable erection stage is assumed to occur just prior to the closure of the span, then the slope at the end of the overhangs

may also be taken as zero.

Regarding the variation of the drag coefficient, it is worthwhile mentioning that, for usual bridge decks and in the absence of experimental data, the ECCS document refers to a linear relationship between C_D and the parameter D/B (where D and B are the depth and the width of the deck, respectively). The EC1 also refers to a linear variation of C_D ; however, this linearity is not upon D/B but rather on its inverse, B/D , and extends up to B/D equal to 4 or 5, depending on the type of deck.

In the following, the ratio between the values that D and C_D present over the pier and at the tip of the overhangs is labelled by Ψ_D and Ψ_C , respectively, and an additional coefficient (Ψ) is defined as $\Psi = \Psi_D \Psi_C$.

To assess the influence of variable deck geometry on the gust factors, two sets of three different situations were considered. The situations in each set have a common Ψ -value, namely $\Psi = 3.0$ and $\Psi = 6.0$, and the parabolic variations were assumed to have zero slope at $s = L/2$. The situations considered in the set $\Psi = 3.0$ were as follows :

- 1) $D(s)$ is parabolic and $C_D(s)$ is constant ($\Psi_D = 3.0$);
- 2) both $D(s)$ and $C_D(s)$ are parabolic, with $\Psi_D = 2.5$ and $\Psi_C = 1.2$;
- 3) both $D(s)$ and $C_D(s)$ are linear, with $\Psi_D = 2.5$ and $\Psi_C = 1.2$.

In the same way, the following situations were considered in the set $\Psi = 6.0$:

- 4) $D(s)$ is parabolic and $C_D(s)$ is constant ($\Psi_D = 6.0$);
- 5) both $D(s)$ and $C_D(s)$ are parabolic, with $\Psi_D = 4.0$ and $\Psi_C = 1.5$;
- 6) both $D(s)$ and $C_D(s)$ are linear, with $\Psi_D = 4.0$ and $\Psi_C = 1.5$.

The variation of the deck geometry has an obvious effect on the mean response (either in the alongwind effect, μ_F , or in the torsional one, μ_{Th}). The remaining influence on the response can be analysed by looking at the ratio $J(\phi) / \gamma_m$ (or $J(\phi) / \gamma_{mh}$), as the background and the resonant components are directly proportional to this parameter.

Figs. 3 and 4 illustrate the values of $J(\phi) / \gamma_{mF}$ and of $J(\phi) / \gamma_{mTh}$ for the case of a deck with constant cross section (labelled by $\Psi = 1.0$) and for the two sets of variable geometry decks that were referred previously. The results obtained in each set for the three situations are practically coincident, with differences hardly noticeable at the scale of the figure, and so the values were grouped in a single curve (defined by the average values).

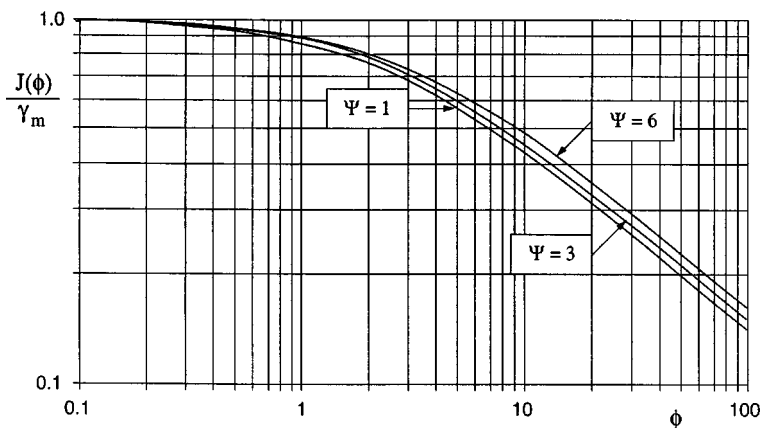


Fig. 3 Comparison of $J(\phi) / \gamma_m$ for different values of Ψ (bending)

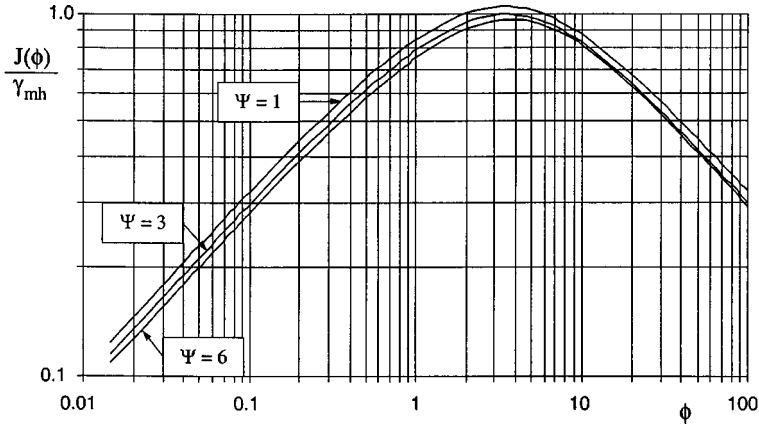


Fig. 4 Comparison of $J(\phi) / \gamma_{mh}$ for different values of Ψ (torsion)

The important conclusion that can be drawn from Figs. 3 and 4 is that the ratios $J(\phi) / \gamma_m$ are little affected by the deck cross section being variable. The condition $\Psi = 6.0$ covers practically all the cantilever bridges built so far. Thus, for practical situations of variable geometry decks, the ratio $J(\phi) / \gamma_m$ (and thus the gust factor ϕ) either for the net drag force on the deck or for the torsional effects can be evaluated as if the deck were constant.

The error involved in this approximation may be disregarded for design purposes - in the cases considered for the set $\Psi = 3.0$, for instance, the differences did not exceed 7% of the exact value in the alongwind case and 9% in the torsional one (less than 6% in the range $2 < \phi < 6$); for the set $\Psi = 6.0$, the maximum difference was around 14% in the alongwind case and 15% for the torsional effect (less than 10% in the range $2 < \phi < 6$). It should be referred that the differences to the exact values are small but show opposite trends, as they are conservative for torsion but are not conservative for bending.

Any torsional moment on the pier can be viewed as the result of a concentrated drag force acting on the deck at a proper distance from the axis of the pier. Denoting by μ_{Fh} the mean value of the drag force that acts over only one of the overhangs, the mean torsional moment μ_{Th} can be evaluated through :

$$\mu_{Th} = e_c \mu_{Fh} \quad (31)$$

where e_c is an equivalent eccentricity. The expression for e_c is simply :

$$e_c = \frac{\mu_{Th}}{\mu_{Fh}} = \frac{\int_0^{L/2} D(s) C_D(s) s \, ds}{\int_0^{L/2} D(s) C_D(s) \, ds} \quad (32)$$

The values taken by the non-dimensional eccentricity $\chi = e_c / (L / 2)$ for a range of Ψ_D and Ψ_C -values (considering parabolic variations with zero slope at mid-span) are depicted in Fig. 5. If the cross section of the deck is constant, the eccentricity e_c is obviously equal to half the length of each overhang (i.e., $\chi = 0.5$). For decks with variable cross section, χ decreases as the relative variation of depth increases.

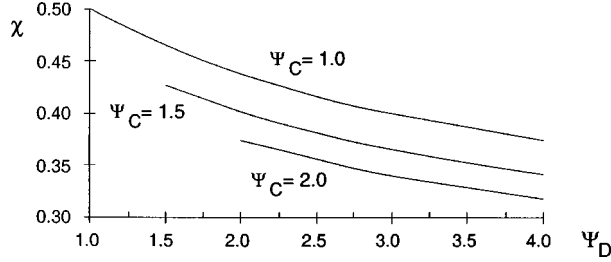


Fig. 5 Non-dimensional eccentricity

Several remarks should be made about the procedure to evaluate the buffeting effects that was described. The first one is that the results can be rather sensitive to the structural damping, depending on the relative importance of the resonant effects; the influence of damping should be investigated by considering a suitable range of variation. The decay coefficient C_r constitutes another source of uncertainty and, regarding the torsional effects, the maximum structural response does not necessarily correspond to a minimum value of C_r . Once again, a suitable range of variation may be considered, such as the range given in Solari 1987 (Eq. 20).

A final remark is that the procedure outlined does not cover all the aerodynamic phenomena that may contribute to the structural response, such as the flexural effects in the crosswind plane, the pressure correlation on the windward and leeward sides of the deck and the effects of wake excitation (Solari 1988). The assumption that the bridge is a line-like structure also precludes considering the vertical correlation of the pressures along the depth of the deck. Albeit these limitations, it is the authors' belief that the method is accurate enough and rather suitable to design practice.

5. Correspondence with the NBCC format

The background and resonant standard deviations can be expressed in the format of Eqs. (5), that are rewritten below in brackets, or in the format adopted in NBCC 1990 :

$$\sigma_b = \mu \sqrt{\frac{K}{C_{eH}}} B \quad \left[= \mu(2I_{u.ref}) \frac{1}{\gamma_m} \sqrt{J_b^2(\phi_b)} \right] \quad (33a)$$

$$\sigma_r = \mu \sqrt{\frac{K}{C_{eH}} \frac{SF}{\delta/(2\pi)}} \quad \left[= \mu(2I_{u.ref}) \frac{1}{\gamma_m} \sqrt{\pi^2 / (2\delta) E(z_{ref}, f_e) |J_r(\phi_r)|^2} \right] \quad (33b)$$

The variables K and C_{eH} , called the surface roughness factor and the exposure factor at height H , are defined in NBCC for each terrain category but, for the present purpose, only the ratio K/C_{eH} is important. The variable F is called the gust energy ratio and S is the size reduction factor. The term B corresponds to the background turbulence effects and the term SF/δ is associated with the resonant component. If the following definitions are considered :

$$\frac{K}{C_{eH}} = 16 \left(\frac{U^*}{U_{ref}} \right)^2 = \frac{4}{\beta} (2I_{u.ref})^2 \quad (34)$$

$$F = \frac{f_e S_u(z_{ref}, f_e)}{4(U^*)^2} = \frac{\beta}{4} E(z_{ref}, f_e) \quad (35)$$

where U^* denotes the friction velocity and β is defined such that $\sigma_u^2(z_{ref}) = \beta (U^*)^2$, the equivalence between the NBCC format and that of Eqs. (5) is attained with :

$$B = \frac{\beta J_b^2(\phi_b)}{4 \gamma_m^2} \quad (36)$$

$$S = \frac{\pi J_r^2(\phi_r)}{4 \gamma_m^2} \quad (37)$$

The NBCC format can be applied for both the alongwind and the torsional effects. If the torsional moment is considered, for instance, then the term μ in Eqs. (33) should be interpreted as μ_{Th} and the term γ_m in Eqs. (36) and (37) corresponds to γ_{mTh} .

If the gust factor in a variable geometry deck is evaluated without considering any variation of the deck geometry, as it was argued before, then, for the drag on the deck, $\gamma_{mF} = 1$ and the J^2 - functions are given by Eq. (23) (Fig. 2); in the same way, for the torsional moment, $\gamma_{mTh} = 1/4$ and the J^2 - functions are given by Eq. (29).

6. Combination of torsional and bending effects

The torsional moments (T) induced on a pier by the wind action during double cantilever erection stages occur in association with bending effects, namely with alongwind shear forces (V) and bending moments (M). Thus, the analysis of the joint effects should be considered in the design of the pier. The shear force on the alongwind walls (V_w) of a pier with hollow rectangular cross section (Fig. 6) is considered to illustrate the combination of bending and torsional effects.

The shear force in the alongwind walls is an important structural response - the design of the transverse reinforcement on a concrete pier, for instance, depends directly on V_w . Assuming the Bredt's model for the torsional behavior of the cross section, the combination T - V leads to the following expression for V_w :

$$V_w(z) = \frac{V(z)}{2} \pm \frac{T}{2b(z)} \quad (38)$$

where $b(z)$ is the distance between the centrelines of the alongwind walls. Thus, V_w at each cross section of the pier corresponds to a linear combination of V and T .

The shear force at the top of the pier is equal to the net drag force over the whole deck (F) and

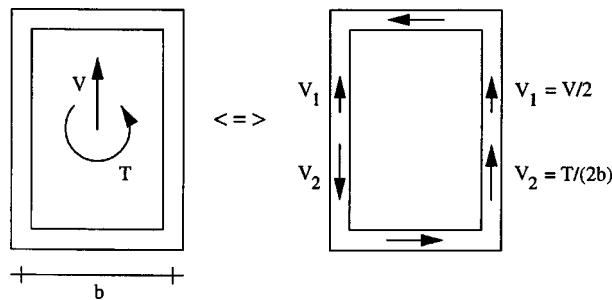


Fig. 6 Hollow rectangular section under torsion+shear

increases to the bottom due to the drag on the pier itself. In the following, for the sake of clarity in the illustration of the joints effects and without compromising the keypoints that will be referred to, the drag on the pier will be neglected and it is assumed that $b(z)$ is constant. Thus, the global shear force on the pier is simply $V(z) = F$ (= constant).

As $\mu_T = 0$, the mean value of V_w is given by :

$$\mu_{V_w} = \frac{\mu_F}{2} = \mu_{Fh} \quad (39)$$

Regarding the resonant component of σ_{V_w} , both the alongwind bending and the torsional modes of vibration (with frequencies denoted by f_b and f_t , respectively) contribute to the fluctuations of V_w . As it was stated before, no modal coupling is considered (which is acceptable if f_b and f_t are not too close). Thus, the resonant variance of the V_w -fluctuations is obtained through :

$$\sigma_{r.V_w}^2 = (1/2)^2 \sigma_{r.F}^2 + (1/(2b))^2 \sigma_{r.T}^2 \quad (40)$$

Because the g_b -function for F is even ($g_{b1}(s) = 1$) and the g_b -function for T is odd ($g_{b2}(s) = 2s/L$) the background components of the F and T contributions to the V_w fluctuations also behave as uncorrelated, so that the linear combination of variances expressed by Eq. (40) also applies to $\sigma_{b.V_w}^2$. The demonstration is given in Appendix A.

Thus, the total variance of V_w is given by :

$$\sigma_{V_w}^2 = (1/2)^2 \sigma_F^2 + (1/(2b))^2 \sigma_T^2 \quad (41)$$

Considering that $\mu_{Th} = e_c \mu_{Fh}$ (Eq. 31) and that $\mu_F = 2\mu_{Fh}$, the expressions for σ_F and σ_T may be written in the form :

$$\sigma_F = \mu_{Fh} (2I_{u.ref}) \frac{2}{\gamma_{mF}} \sqrt{v_{bF} + v_{rF}} \quad (42)$$

$$\sigma_T = \mu_{Fh} (2I_{u.ref}) \frac{e_c}{\gamma_{mTh}} \sqrt{v_{bT} + v_{rT}} \quad (43)$$

As it was stated before, it is possible to take $\gamma_{mF} = 1$ and to evaluate the variances v_{bF} and v_{rF} from the J^2 -function given by Eq. (23); in the same way, it is possible to consider $\gamma_{mTh} = 1/4$ and to evaluate the variances v_{bT} and v_{rT} from the J^2 -function given by Eq. (29). Besides, $\mu_{Fh} = \mu_{V_w}$. Thus, the following expression is derived from Eqs. (42-43) :

$$\sigma_{V_w} = \mu_{V_w} (2I_{u.ref}) \sqrt{(v_{bF} + v_{rF}) + (2e_c/b)^2 (v_{bT} + v_{rT})} \quad (44)$$

Fig. 2 illustrates that the background-bending variance (v_{bF}) is always larger than the torsional one (v_{bT}). In fact, for a same ϕ_b -value and in the range $3 < \phi < 10$, for instance, the J^2 -function for bending is about 4 to 7 times the J^2 -function for torsion. In the same way, regarding the resonant variances, v_{rF} is usually larger than v_{rT} (the difference between v_{rF} and v_{rT} may be even higher than between the background variances, depending upon f_b and f_t). However, since the eccentricity e_c is typically much larger than the cross dimension of the pier (i.e., $e_c/b \gg 1$), the torsional contribution to σ_{V_w} in hollow rectangular piers usually becomes the predominant term.

To obtain the characteristic value of the joint effect V_w (through Eq. 4, with κ given by Eq. 21), the zero-upcrossing frequency (ν) may be taken as a weighted average of the structural frequencies that are involved. Taking into account Eq. (44), that describes the distinct components of variance, the

following expression may be considered in this case :

$$v^2 = \frac{v_{rF}f_b^2 + (2e_c/b)^2 v_{rT}f_t^2}{(v_{bF} + v_{rF}) + (2e_c/b)^2 (v_{bT} + v_{rT})} \quad (45)$$

When the total variance of a combined response (such as $R = a_1R_1 + a_2R_2$) is a linear combination of the variances of the individual effects, such as in the present case, the characteristic value of the combined response is given by :

$$R_k = (a_1\mu_{R1} + a_2\mu_{R2}) + \kappa_R \sqrt{a_1^2\sigma_{R1}^2 + a_2^2\sigma_{R2}^2} \quad (46)$$

Despite its theoretical inconsistency, it is interesting to refer to a simplified approach that consists of estimating the characteristic value of a combined response as a linear combination of the characteristic values of the individual effects (R_{k1} and R_{k2}), i.e. :

$$R_k^* = a_1R_{k1} + a_2R_{k2} \quad (47)$$

Within this approach, if the individual gust factors for R_1 and R_2 are taken equal to κ_R (in fact, the differences are usually small, since the variation of κ with frequency is slow), it follows that :

$$R_k^* = (a_1\mu_{R1} + a_2\mu_{R2}) + \kappa_R (a_1\sigma_{R1} + a_2\sigma_{R2}) \quad (48)$$

The comparison between Eqs. (46) and (48) reveals that $R_k^* > R_k$, i.e., the simplified method leads to a conservative estimate of the combined response.

Finally, it is worthwhile discussing the influence of the decay coefficient (C_r) in the joint analysis of torsion and alongwind bending. In fact, the maximum torque is obtained with $\phi \approx 3.4$; on the other hand, the lower is C_r the higher become the alongwind effects. Thus, the design situation should reflect a compromise between the different role played by C_r .

Once a certain range of variation of C_r is assumed for design purposes, such as the range proposed by Solari (Eq. 20), let the minimum and maximum C_r - values be denoted by C_{rm} and C_{rM} , respectively. The values of ϕ_r that correspond to the torsional frequency and to these extreme C_r - values may also be defined (and denoted by ϕ_{rmt} and ϕ_{rMt} , respectively). Assuming that the resonant contributions dominate over the background ones, the following situations may then occur in the analysis of the joint effects :

- if $\phi_{rmt} > 3.4$, the assumption $C_r = C_{rm}$ may be adopted for design, as the structural response would certainly decrease if higher values were considered for C_r ;
- if $\phi_{rmt} \leq 3.4 \leq \phi_{rMt}$, the combined response should be assessed for C_r - values in the range $[C_{rm}, 3.4 U_{ref} / (f_t L)]$;
- if $\phi_{rMt} < 3.4$, it is advisable to consider the whole range $[C_{rm}, C_{rM}]$, in order to attain the most unfavourable situation.

7. Example of application

The procedure described above is applied to the bridge that crosses the Douro River at Régua, Portugal. This structure was designed by Eng. Armando Rito and its construction finished in 1997. The main span of the bridge is 180.0m long and the piers are 87.0 m high. The deck is a prestressed reinforced concrete box girder and presents a parabolic variation of depth between 4.0 m at mid-span and 12.0 m over the piers. At the erection stage just prior to the closure of the main span, the

structure presented $L = 175$ m, $f_b = 0.304$ Hz and $f_t = 0.122$ Hz.

The drag coefficient of the deck is assumed to have a parabolic variation between $C_D = 1.25$ at mid-span and $C_D = 1.75$ at the connection to the piers. The reference value of the structural damping is taken as $\delta_s = 0.05$ and the aerodynamic damping for each mode of vibration (with generic frequency f_e) is estimated by :

$$\delta_a = \frac{\rho U D C_D}{2 m f_e} \quad (49)$$

It is assumed that the structural parameter $m / (D.C_D)$ is constant along the entire span. The value $m / (D.C_D) = 6400$ kg/m², that pertains to the tip of the overhangs, is considered.

The basic wind characteristics are taken from EC1 assuming the terrain category II conditions (typical of farmland with occasional small obstacles) and a reference wind speed $U_{bas} = 20$ m/s (10 min. mean wind speed at 10 m above ground). The lateral length scale of turbulence is taken as $L_u^y = (1/3)L_u^x$ (Dyrbye and Hansen 1996). The input parameters and the corresponding results for the torsional moment on the pier are listed in Table 1. The values shown for κ (and for φ) correspond to a duration $T = 10$ minutes. The values of the NBCC coefficients are also presented at the bottom of the table.

All the gust factors shown in Table 1 have been obtained as if the deck had a constant cross section.

The gust factor obtained for the basic situation (denoted by Case 1) is equal to 2.37. If the parabolic variations of the depth and of the drag coefficient are taken into account (considering $\Psi_D = 12.0/4.0 = 3.0$ and $\Psi_C = 1.75/1.25 = 1.4$), the gust factor decreases from 2.37 to 2.22. The error involved is conservative and of only 7%, that illustrates the validity of considering a constant cross section in design practice.

In order to assess the influence of some parameters in the structural response, three other cases were considered. In each case all the data are equal to those of Case 1 except for one parameter. The influence of the structural damping is illustrated in Case 2: if $\delta_s = 0.10$ is considered, for instance, the gust factor is reduced from 2.37 to 1.90.

The value $\phi_r = 8.7$ in Case 1 corresponds to $C_r = 11.5$, which is in accordance to EC1 but is beyond the range of values for which the joint acceptance function is maximum (vd. Fig. 2). In Case 3, the decay coefficient C_r is taken as the lower limit of the range proposed by Solari (i.e., $C_r = 5.0 \times (175/87)^{0.25} = 6.0$) and $\phi_r = 4.5$ is obtained. As this value is closest to the ‘‘critical’’ range for torsion ($3 < \phi_r < 4$), the gust factor becomes higher than in Case 1 (2.65 instead of 2.37). If the value $\phi_r = 3.4$ is considered (the value at which J_r^2 is maximum), the gust factor becomes even higher; in this case, the result $\varphi = 2.68$ would then be obtained.

The significant height of the piers and the long span of this structure (in terms of frame bridges) make it rather flexible during the erection stages, as the low structural frequencies reveal. For this reason, the resonant effects of the wind gusts are much more important than the background turbulence effects (in Case 1, for instance, $v_{r,T} = 0.441$ is 87% of total variance). Case 4 illustrates the importance of the structural frequency in the response: if a larger value is given to f_t (namely 0.3 Hz), the relative contribution of the resonant effects becomes lower, as well as the gust factor (1.75 instead of 2.37).

In all the cases shown, the zero-upcrossing frequency (ν) of the torsional response is very close to the structural frequency (f_t). This fact is typical in flexible structures and rather small differences would be obtained if ν had been identified directly with f_t instead of using Eq. (22) (in Case 1, for instance, the gust factor would change from 2.37 to 2.39).

Regarding the alongwind effects, the main results obtained by the same methodology for the net

Table 1 Input parameters and results for torsional effects

INPUT	Case 1	Case 2	Case 3	Case 4
Basic wind speed, U_{bas} [m/s]	20	"	"	"
Roughness length, z_o [m]	0.05 (*)	"	"	"
Terrain factor, k_T	0.19 (*)	"	"	"
Exponent for scale of turbulence, ε	0.26 (*)	"	"	"
Air density, ρ [kg/m ³]	1.25	"	"	"
Total length of the structure, L [m]	175	"	"	"
Height of the deck above ground, H [m]	87	"	"	"
Reference depth (tip of the arms), D_{ref} [m]	4	"	"	"
Reference drag coefficient, $C_{D.ref}$	1.25	"	"	"
Torsional frequency, f_t [Hz]	0.122	"	"	0.3
Structural damping, δ_s	0.05	0.10	0.05	0.05
Equivalent mass per unit area, (m/D) [kg/m ²]	8000	"	"	"
Decay coefficient, C_r	11.5 (*)	"	6.0	11.5
RESULTS	Case 1	Case 2	Case 3	Case 4
Wind speed at deck level, $U_{ref} = k_T \ln(H/z_o) U_{bas}$ [m/s]	28.4 (*)	"	"	"
Intensity of turbulence, $I_{u.ref} = 1/\ln(H/z_o)$	0.134 (*)	"	"	"
Longitudinal scale of turbulence, $L_u^x(H) = 300(H/300)^\varepsilon$ [m]	217.4 (*)	"	"	"
Lateral scale of turbulence, $L_u^y(H) = (1/3) L_u^x(H)$ [m]	72.5	"	"	"
ϕ_b Eq. (10)	2.414	"	"	"
Background variance, $v_b = J_b^2(\phi_b)$ Eq. (29) (Fig. 2)	0.066	"	"	"
ϕ_r Eq. (19)	8.659	"	4.518	21.293
Joint acceptance function, $J_r^2(\phi_r)$ Eq. (29) (Fig. 2)	0.052	"	0.067	0.027
$N = f_t \cdot L_u^x / U(H)$	0.936 (*)	"	"	2.301
Non-dimensional spectral density, $E(N) = 6.8N / (1+10.2N)^{5/3}$	0.126 (*)	"	"	0.076
Aerodynamic damping, δ_a Eq. (49)	0.023	"	"	0.009
Total damping, $\delta = \delta_s + \delta_a$	0.073	0.123	"	0.059
Resonant variance, v_r Eq. (13) (with $M_1=M_2$)	0.441	0.261	0.567	0.170
Zero-upcrossing frequency, ν Eq. (22) [Hz]	0.114	0.109	0.115	0.255
Peak factor, κ Eq. (21)	3.105	3.091	3.110	3.354
Gust factor, φ Eq. (26) (with $\gamma_{mh} = 1/4$)	2.37	1.90	2.65	1.75
Mean torsional moment (one overhang), μ_{Th} [kN.m]	14022	"	"	"
Characteristic torsional moment, T_k [kN.m]	33232	26642	37158	24539
NBCC				
Turbulence coefficient, β	6 (*)	"	"	"
Roughness/exposure factor, K / C_{eH} Eq. (34)	0.048	"	"	"
Background factor, B Eq. (36)	1.581	"	"	"
Gust energy ratio, F Eq. (35)	0.188	"	"	0.114
Size reduction factor, S Eq. (37)	0.650	"	0.836	0.338
Gust factor, $\varphi = \kappa \sqrt{K / C_{eH} (B + SF \cdot 2\pi / \delta)}$	2.37	1.90	2.65	1.75

(*) - values taken according to Eurocode 1)

drag force on the deck (F) are summarised in Table 2 (only Case 1 is considered).

To illustrate the joint analysis of alongwind and torsional effects, the pier is assumed to have a

Table 2 Main results for alongwind and torsional effects (Case 1)

	Drag force on the deck (F)	Torsional moment on the pier (T)
f_e (Hz)	0.304	0.122
ϕ_b		2.414
ϕ_r	21.577	8.659
v_b	0.516	0.066
v_r	0.555	0.441
k	3.308	3.105
φ	1.92	2.37
	$\mu_F = 865$ kN	$\mu_{Th} = 14022$ kN.m
	$\sigma_F = 240$ kN	$\sigma_T = 10703$ kN.m
	$F_k = 1660$ kN	$T_k = 33232$ kN.m

hollow rectangular section with $b(z) = 6.00$ m and the shear force in the alongwind walls (V_w) is considered (“pier-drag” is neglected).

According to Eq. (44), the equivalent eccentricity e_c must be evaluated in order to assess σ_{V_w} . From Fig. 5, for $\Psi_D = 3.0$ and $\Psi_C = 1.4$, $\chi = e_c / (L/2) \approx 0.37$. Thus, $e_c \approx 0.37 \times (175/2) = 32.4$ m and $e_c / b \approx 5.4$. The same result can be obtained through $e_c = \mu_{Th} / (\mu_F / 2)$.

The main results obtained for V_w in Case 1 are presented in Table 3. The value obtained for $(v_{bF} + v_{rF})$ is almost the double of $(v_{bT} + v_{rT})$; however, as $e_c / b = 5.4 \gg 1$, the torsional contribution to σ_{V_w} becomes clearly predominant over the alongwind one (in fact, the torsional contribution corresponds to 98% of the total V_w -variance). This fact is reflected by the high value of the gust factor for V_w , namely $\varphi = 7.47$.

To illustrate the influence of “pier-drag”, if the cross section of the pier is considered with a crosswind outer dimension equal to 6.60 m and with a drag coefficient of 1.7, the value obtained for the total “pier-drag” due to mean wind speed is 329 kN (38% of μ_F) and the corresponding bending moment at the base of the pier is only 19% of the moment $\mu_F H$. Thus, if the “pier-drag” had been considered in the joint analysis, the torsional effects would still clearly predominate on V_w and the characteristic response ($V_{w,k}$) would be little affected.

Finally, if the characteristic response is estimated through Eq. (47), the result would be $V_{w,k}^* = (1/2)F_k + 1/(2 \times 6.0)T_k = 3599$ kN. As it was referred before, this is a conservative estimate of the characteristic response ($V_{w,k} = 3229$ kN).

Table 3 Main results for the combined response V_w (Case 1, with $e_c / b = 5.4$)

$(v_{bF} + v_{rF})$	1.071
$(v_{bT} + v_{rT})$	0.507
$(2e_c / b)^2 (v_{bT} + v_{rT})$	59.092
σ_{V_w} / μ_{V_w} (Eq. 44)	2.08
v (Eq. 45)	0.116 Hz
κ (Eq. 21)	3.112
φ (Eq. 6)	7.47
$\mu_{V_w} = \mu_F / 2$ (Eq. 39)	432 kN
$V_{w,k} = \varphi \mu_{V_w}$ (or Eq. 46)	3229 kN

8. Conclusions

The torsional effects induced on bridge piers by unbalanced wind buffeting on the deck during double cantilever erection stages may be significant and should be considered in the design of such bridges. The Sir Benjamin Baker's rule-of-thumb ($\phi = 1$) may give a reasonable estimate of such effects if the torsional frequency is high (namely for typical short-span bridges, say L less than 60 to 80 m) but it is rather incorrect for flexible cantilever bridges ($\phi \gg 1$).

The evaluation of the gust factor on cantilever bridges that present a deck with variable depth may be performed as if the depth were constant. In fact, neither the variation of the depth nor the variation of the drag coefficient have any relevant influence on the gust factor for alongwind bending or for torsional effects. However, it should be clear that the mean response must be evaluated by considering the real geometry of the deck.

The combination of alongwind and torsional effects should be considered in the design of the piers. The importance of the torsional component was illustrated for the case of shear in the alongwind walls of a pier with hollow rectangular cross section.

The method illustrated in this paper is suitable for design practice and for implementation in structural codes.

References

- ASCE Committee on Loads and Forces on Bridges (1982), "Bridge loading: research needed", *J. Struct. Div.*, ASCE, **108**(5), 1012-1020.
- Davenport, A. (1967), "Gust loading factors", *J. Struct. Div.*, ASCE, **93**(3), 11-34.
- Davenport, A. (1994), "The consistent safety of long span bridges against wind with special reference to Normandy Bridge", *Proc. of Congress on Cable-Stayed and Suspension Bridges*, AFPC, Deauville, **2**, 3-14.
- Dyrbye, C. and Hansen, S. (1996), *Wind Loads on Structures*, John Wiley & Sons.
- EC1 - Eurocode 1 (1995), "Basis of design and actions on structures. Part 2.4: Actions on structures - Wind actions", *European Prestandard ENV 1991-2-4*.
- ECCS - European Convention for Constructional Steelwork (1989), "Recommandations pour le calcul des effets du vent sur les constructions", *Construction Métallique*, **1**.
- Foutch, D. and Safak, E. (1981), "Torsional vibration of along-wind excited structures", *J. Eng. Mechs. Div.*, ASCE, **107**, 323-337.
- NBCC - National Building Code of Canada (1990), National Research Council of Canada.
- Revelo, C., Guillen, C., Chauvin, A., Mejia, M., Paulik, L., Arguelles, G. and Aguilar, J. (1994), "The four cable-stayed bridges of the Mexico-Acapulco highway", *Proc. of Congress on Cable-Stayed and Suspension Bridges*, AFPC, Deauville, **1**, 351-360.
- Solari, G. (1987), "Turbulence modelling for gust loading", *J. Struct. Eng.*, ASCE, **113**(7), 1550-1569.
- Solari, G. (1988), "Equivalent wind spectrum technique: Theory and applications", *J. Struct. Eng.*, ASCE, **114**(6), 1303-1323.
- Solari, G. (1993), "Gust buffeting. II: Dynamic alongwind response", *J. Struct. Eng.*, ASCE, **119**(2), 383-398.
- Tang, M. (1994), "Cable-stayed bridges in the United States", *Proc. of Congress on Cable-Stayed and Suspension Bridges*, AFPC, Deauville, **1**, 213-224.
- Wheeler, K., Lothringer, S. and Bennett, M. (1994), "Glebe Island Bridge Australia's new cable-stayed bridge", *Proc. of Congress on Cable-Stayed and Suspension Bridges*, AFPC, Deauville, **1**, 307-315.

Appendix A - Background variance of a combined response

Consider a structural response (R) that results from a linear combination of two other responses (R_1 and R_2), i.e. :

$$R(s) = a_1 R_1(s) + a_2 R_2(s) \quad (\text{A.1})$$

where a_1 and a_2 are constants. In the case of a horizontal line-like structure with constant cross section, the Eq.(5a) corresponds to :

$$\sigma_{b,R}^2 = [\rho U(H) D C_D \sigma_u(H)]^2 \int_0^L \int_0^L I_R(s_1) I_R(s_2) \rho_u(r) ds_1 ds_2 \quad (\text{A.2})$$

where $r = |s_1 - s_2|$. Considering that $I_R(s) = a_1 I_{R1}(s) + a_2 I_{R2}(s)$, and omitting subscript R from the background variances of the responses, the following expression may be derived :

$$\begin{aligned} \sigma_b^2 = & a_1^2 \sigma_{b1}^2 + a_2^2 \sigma_{b2}^2 + a_1 a_2 [\rho U(H) D C_D \sigma_u(H)]^2 (I_{R1.ref} I_{R2.ref}) \\ & \times \int_0^L \int_0^L \left[\frac{I_{R1}(s_1) I_{R2}(s_2)}{I_{R1.ref} I_{R2.ref}} + \frac{I_{R2}(s_1) I_{R1}(s_2)}{I_{R2.ref} I_{R1.ref}} \right] \rho_u(r) ds_1 ds_2 \end{aligned} \quad (\text{A.3})$$

The generalisation of this expression for any line-like structure is straightforward. The result is :

$$\sigma_b^2 = a_1^2 \sigma_{b1}^2 + a_2^2 \sigma_{b2}^2 + [\rho U_{ref} D_{ref} C_{D.ref} \sigma_{u.ref} I_{R.ref} L]^2 J_{b,12}^2 \quad (\text{A.4})$$

where $I_{R.ref}^2$ and $J_{b,12}^2$ are defined through :

$$I_{R.ref}^2 = (a_1 I_{R1.ref} a_2 I_{R2.ref}) \quad (\text{A.5})$$

$$J_{b,12}^2 = \frac{1}{L^2} \int_0^L \int_0^L [g_{b1}(s_1) g_{b2}(s_2) + g_{b2}(s_1) g_{b1}(s_2)] \rho_u(r) ds_1 ds_2 \quad (\text{A.6})$$

Just like the double integral in Eq. (7) can be solved through Eqs. (11), (12), the double integral in Eq. (A.6) can be solved by the following procedure (the demonstration is similar to the one given in Dyrbye and Hansen 1996 for a single g_b - function):

$$J_{b,12}^2 = \frac{1}{L} \int_0^L G_{b,12}(r) \rho_u(r) dr \quad (\text{A.7})$$

$$G_{b,12}(r) = \frac{2}{L} \int_0^{L-r} [g_{b1}(s) g_{b2}(s+r) + g_{b2}(s) g_{b1}(s+r)] ds \quad (\text{A.8})$$

If the origin of the s -axis is located at the middle of the structure and not at one of the tips, the limits of integration in Eq. (A.8) change from $(0, L-r)$ to $(-L/2, L/2-r)$. Taking into account that :

$$\int_{-L/2}^{L/2-r} [g_{b2}(y) g_{b1}(y+r)] dy = - \int_{L/2-r}^{-L/2} [g_{b2}(-s-r) g_{b1}(-s)] ds = \int_{-L/2}^{L/2-r} [g_{b1}(-s) g_{b2}(-s-r)] ds \quad (\text{A.9})$$

the Eq. (A.8) can be rewritten in the form :

$$G_{b,12}(r) = \frac{2}{L} \int_{-L/2}^{L/2-r} [g_{b1}(s) g_{b2}(s+r) + g_{b1}(-s) g_{b2}(-s-r)] ds \quad (\text{A.10})$$

It is clear that if one of the g_b - functions is even and the other is odd, the corresponding $G_{b,12}$ - function is zero and so is $J_{b,12}^2$. Thus, the background components of the R_1 and R_2 contributions to R behave as uncorrelated, in the sense that :

$$\sigma_b^2 = a_1^2 \sigma_{b1}^2 + a_2^2 \sigma_{b2}^2 \quad (\text{A.11})$$